INFLUENCE OF NANO-SIZED COBALT OXIDE ADDITIONS ON THE STRUCTURAL AND ELECTRICAL PROPERTIES OF NICKEL-MANGANITE-BASED NTC THERMISTORS

VPLIV DODATKA NANODELCEV KOBALTOVEGA OKSIDA NA ZGRADBO IN ELEKTRIČNE LASTNOSTI NTC TERMISTORJEV NA OSNOVI NIKLJEVEGA MANGANITA

Gökhan Hardal, Berat Yüksel Price

Istanbul University, Engineering Faculty, Metallurgical and Materials Engineering Department, Avcılar, Istanbul, Turkey
berat@istanbul.edu.tr

The structural and electrical properties of $NiMn_2O_4$ and $Ni_{0.5}Co_xMn_{2.5-x}O_4$ (where $x = 0.5$, 0.8 and 1.1) NTC thermistors have been investigated. The samples, prepared by conventional ceramic processing techniques, were calcinated at 900 °C for 2 h and then sintered at 1100 °C and 1200 °C for 5 h. The cubic spinel phase was observed by XRD analysis in the $NiMn_2O_4$ and $Ni_{0.5}Co_{0.8}Mn_{1.7}O_4$ samples sintered at 1100 °C for 5 h. The sintering at 1200 °C resulted in much denser microstructures with a larger grain size. The room-temperature electrical resistivity (ρ_{25}) and material constant (B) value of the $NiMn_2O_4$ sample sintered at 1100 °C were 7710 Ω cm and 3930 K, respectively. The electrical resistivity of the samples decreased significantly with the addition of Co_3O_4. The $B_{25/85}$ values of the $Ni_{0.5}Co_xMn_{2.5-x}O_4$ (where $x = 0.5$, 0.8 and 1.1) samples sintered at 1100 °C were found to be 3820 K, 3525 K and 3270 K, respectively.

Keywords: cobalt oxide, electrical properties, microstructure, NTC thermistor

Preiskovana je bila zgradba in električne lastnosti $NiMn_2O_4$ in $Ni_{0.5}Co_xMn_{2.5-x}O_4$ (kjer je $x = 0,5$, 0,8 in 1,1) NTC termistorjev. Vzorci, pripravljeni po običajni tehniki priprave keramike, so bil kalcinirani 2 h na 900 °C in potem 5 h sintrani na 1100 °C in 1200 °C. Kubična špinelna faza je bila opažena pri XRD-analizi, v vzorcih $NiMn_2O_4$ in $Ni_{0.5}Co_{0.8}Mn_{1.7}O_4$, sintranih 5 h na 1100 °C. Sintranje na 1200 °C je povzročilo mnogo bolj gosto mikrostrukturo z večjimi zrni. Vrednosti za električno upornost pri sobni temperaturi (ρ_{25}) in materialne konstante (B) vzorca $NiMn_2O_4$, sintranega na 1100 °C, sta bili 7710 Ω cm in 3930 K. Električna upornost vzorcev se je občutno zmanjšala po dodatku Co_3O_4. Vrednosti $B_{25/85}$ pri vzorcih $Ni_{0.5}Co_xMn_{2.5-x}O_4$ (kjer je bil $x = 0,5$, 0,8 in 1,1) sintranih na 1100 °C so bile: 3820 K, 3525 K in 3270 K.

Ključne besede: kobaltov oksid, električne lastnosti, mikrostruktura, NTC termistor

1 INTRODUCTION

Sensors for monitoring and controlling temperature are very important, not only in our daily life but also in many industrial and laboratory applications such as aerospace and automotive industries, circuit compensation, cryogenic systems etc.[1,2] NTC thermistors are useful for precision temperature measurements as their resistance decreases with increasing temperature.[3] The most extensively used negative temperature coefficient (NTC) thermistor materials are nickel-manganite-based semiconducting materials which exhibit the spinel-type crystal structure with the general formula AB_2O_4.[4] In the spinel structure, there are two sites available for the cations, i.e., the tetrahedral site, A-site, and the octahedral site, B-site. The distribution of the ions over the sites is as follows: Mn^{3+} will predominantly occupy the B-site, while Mn^{2+} will be placed on the A-site and the majority Ni^{2+} will go to the B-site.[5] The electrical resistivity, ρ, of NTC thermistors varies exponentially with temperature, T, by the well-known Arrhenius equation $\rho = \rho_o \exp(B/T)$, where ρ_o is the resistivity of the material at infinite temperature and B is a constant, which is a measure of the sensitivity of the materials over a given temperature.[6] The material constant B, can be calculated using Equation (1):

$$B_{\frac{T1}{T2}} = \frac{\ln \rho_1 - \ln \rho_2}{\frac{1}{T_1} - \frac{1}{T_2}} \qquad (1)$$

where ρ_1 and ρ_2 are the electrical resistivity at temperatures T_1 and T_2, respectively. The activation energy E_a can also found by the equation $B = E_a/k_B$, where k_B is the Boltzmann constant.[7]

The electrical properties of nickel-manganite-based NTC thermistors closely depend on the ratio of the compositions (type and amount of additives), initial particle size of raw materials and processing conditions (selected synthesis method, calcination and sintering temperature, sintering time etc.). Attainment of high-density, controlled-grain-size microstructures and appropriate dimensional designs are important factors in good sensor design.[8] Previous studies have been focused on the effect

of composition ratios and different production routes on the electrical properties of various metal-oxide-doped NTC thermistors. In this study, nano-sized cobalt-oxide-added, nickel-manganite-based NTC thermistors were fabricated by the solid-state reaction method, the effect of dopant concentration and sintering temperature on the structural and electrical properties of NTC materials were investigated.

2 EXPERIMENTAL PART

The particle size of Co_3O_4 powder was less than 50 nm, purchased from Sigma-Aldrich. NiO (99 % purity, Alfa Aesar), Co_3O_4 (99.5 % purity, Sigma-Aldrich) and Mn_2O_3 (99 % purity, Sigma-Aldrich) powders were weighed according to the compositions of $NiMn_2O_4$ and $Ni_{0.5}Co_xMn_{2.5-x}O_4$ (where x= 0.5, 0.8 and 1.1). The molar ratios of these compositions are given in **Table 1**. The raw powder mixture was ball-milled using ZrO_2 balls as a grinding media with ethyl alcohol in a jar for 5 h. The obtained slurries were dried and powders were calcinated at 900 °C for 2 h. The powders were pressed to form disc-shaped specimens and then sintered at 1100 and 1200 °C for 5 h employing a 360 °C/h heating rate in the air and then cooled naturally in the furnace. The bulk density (ρ, g cm^{-3}) of the sintered samples was calculated from their weights and dimensions. The phases in the sintered samples were determined by X-ray diffraction (XRD, Rigaku D/Max-2200/PC) analysis using Cu-$K\alpha$ radiation at 60 kV/2 kW.

Table 1: Molar ratio of Ni, Mn and Co in all compositions
Tabela 1: Molarno razmerje Ni, Mn in Co v vseh spojinah

Composition code	Ni (moles)	Mn (moles)	Co (moles)
A1	1	2	-
A2	0.5	2	0.5
A6	0.5	1.7	0.8
A10	0.5	1.4	1.1

In order to calculate the lattice parameter of the samples Equation (2) was applied:

$$a = d\sqrt{h^2 + k^2 + l^2} \qquad (2)$$

where h, k and l are the miller indices, a (nm) is the lattice parameter of cubic structure, d is the interplanar spacing of the peaks corresponding to (311).

The volume of the unit cell (V, nm^3) for the cubic system is obtained from Equation (3):

$$V = a^3 \qquad (3)$$

The average values of the crystallite size (D, nm) of the samples were calculated by means of X-ray line broadening method, using the Debye Scherrer formula:

$$D = \frac{0.9\lambda}{\beta \cos \theta} \qquad (4)$$

where 0.9 is a constant related to crystallite shape, λ is the X-ray radiation wavelength in nanometres (nm), β is the full width at half-maximum (FWHM) of the peaks corresponding to (311) and θ is Bragg's angle.[9] The value of β from the 2θ axis of the diffraction profile must be in radians.[10] The microstructure of the samples was observed using scanning electron microscopy (SEM, JEOL, JSM 5600) on fracture surfaces. The sintered samples were coated with silver paste to form electrodes. The electrical resistance was measured in a temperature programmable furnace between 25 °C and 85 °C in steps of 0.1 °C. The material constant, B, the activation energy, E_a, and the sensitivity coefficient, α, values were calculated for the NTC thermistors.

3 RESULTS

The XRD patterns of the $NiMn_2O_4$ and $Ni_{0.5}Co_{0.8}Mn_{1.7}O_4$ samples sintered at 1100 °C for 5 h are given in **Figure 1**. The calculated lattice parameter, unit-cell volume, β, peak position corresponding to (311) and crystallite size of the samples are given in **Table 2**. The XRD analysis of these samples demonstrated only the cubic spinel phase (PDF No: 71-0852). A comparison of the XRD patterns of the sintered samples and the data is given in **Table 2**, the diffraction peaks of the $Ni_{0.5}Co_{0.8}Mn_{1.7}O_4$ sample shifted to higher 2θ angles, and
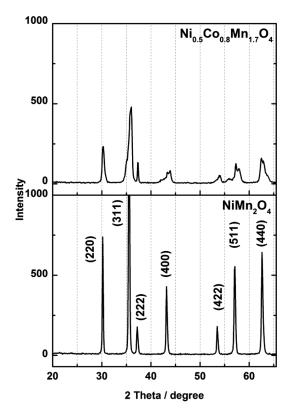

Figure 1: XRD patterns of $NiMn_2O_4$ (A1) and $Ni_{0.5}Co_{0.8}Mn_{1.7}O_4$ (A6) samples in the 2θ range 20–65°
Slika 1: Rentgenogram vzorcev $NiMn_2O_4$ (A1) in $Ni_{0.5}Co_{0.8}Mn_{1.7}O_4$ (A6) v področju 2θ med 20° in 65°
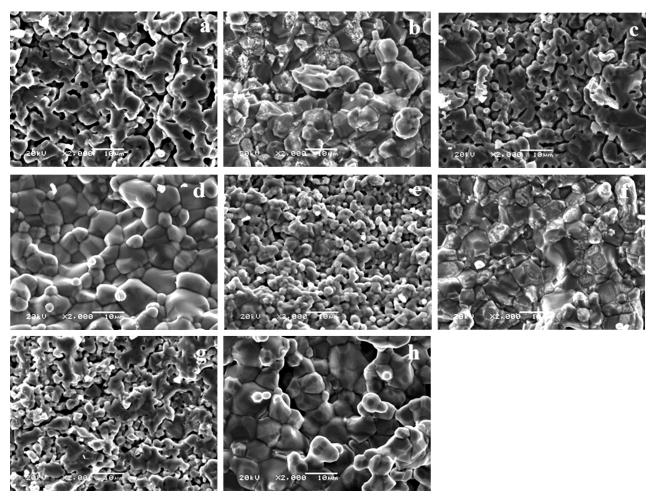
Figure 2: SEM micrographs of sintered samples: A1 a) 1100 °C, b) 1200 °C, A2 c) 1100 °C, d) 1200 °C, A6 e) 1100 °C, f) 1200 °C, A10 g) 1100 °C, h) 1200 °C

Slika 2: SEM-posnetki sintranih vzorcev: A1 a) 1100 °C, b) 1200 °C, A2 c) 1100 °C, d) 1200 °C, A6 e) 1100 °C, f) 1200 °C, A10 g) 1100 °C, h) 1200 °C

as a result the lattice parameters and the unit-cell volume decreased. The value of β increased to 0.7692° and the value of average crystallite size decreased to 10.86 nm.

Table 2: The lattice parameter, unit-cell volume, β, peak position and crystallite size of samples sintered at 1100 °C

Tabela 2: Parameter mreže, prostornina enotne celice, β, položaj vrhov in velikost kristalnih zrn vzorcev sintranih na 1100 °C

Composition	a (L)	V (L^3)	β (311) (°)	2θ (311) (°)	D (nm)
NiMn$_2$O$_4$ (A1)	0.8365	0.585	0.2538	35.6	32.87
Ni$_{0.5}$Co$_{0.8}$Mn$_{1.7}$O$_4$ (A6)	0.8273	0.566	0.7692	36	10.86

The bulk densities of the sintered NiMn$_2$O$_4$ and Ni$_{0.5}$Co$_x$Mn$_{2.5-x}$O$_4$ samples are shown in **Table 3**. The bulk density of the A1 sample sintered at 1100 °C was found to be 4.23 g cm^{-3} and it increased to 4.78 g cm^{-3} when the sample was sintered at 1200 °C. The bulk density of the samples decreased first and then increased with the addition of Co$_3$O$_4$.

Table 3: The bulk density of samples sintered at 1100 °C and 1200 °C for 5 h

Tabela 3: Gostota osnove po 5 urnem sintranju na 1100 °C in 1200 °C

Composition code	ρ (g cm^{-3})	
	1100 °C	1200 °C
A1	4.23	4.78
A2	4.05	4.43
A6	4.27	4.63
A10	4.30	4.72

The SEM micrographs of the A1, A2, A6, A10 samples sintered at 1100 and 1200 °C for 5 h are given in **Figure 2**. It can be seen in this figure that all the samples sintered at 1100 °C had a fine-grained microstructure with most of the pores at the grain boundaries. The grain size of A1 was larger relative to the A2, A6 and A10 samples sintered at 1100 °C. When the sintering temperature was increased to 1200 °C, all the samples had a much denser microstructure and larger grains with a number of small grains on their surface. In addition,
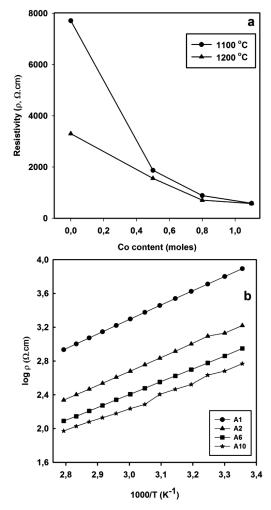
Figure 3: a) The change of resistivity as a function of cobalt content, b) the relationship between $\log \rho$ and $1000/T$ (K^{-1}) for A1, A2, A6 and A10 samples
Slika 3: a) Sprememba upornosti v odvisnosti od vsebnosti kobalta, b) odvisnost med $\log \rho$ in $1000/T$ (K^{-1}) pri vzorcih A1, A2, A6 in A10

the A10 sample had much bigger grains in comparison with the A2 and A6 samples sintered at 1200 °C.

The plot of resistivity versus Co content (moles) and the plots of $\log \rho$ versus $1000/T$ are given in **Figures 3a** and **3b** for all the sintered samples. The plots of $\log \rho$ versus $1000/T$ exhibited a linear dependence in the range 25–85 °C, indicating semiconducting NTC thermistor characteristics. The activation energy, the sensitivity coefficient and the material constant can also be calculated from this plot. The room-temperature electrical resistances, R_{25}, of the A1, A2, A6 and A10 samples sintered at 1100 °C were 1487, 360, 167 and 107 Ω, respectively. For the same sintering temperature, the room temperature electrical resistivity of the A1, A2, A6 and A10 samples were calculated as 7710, 1870, 890 and 590 Ω cm, respectively.

The relationship between the $B_{25/85}$ constant of the samples and the increase in Co$_3$O$_4$ content is given in **Figure 4**. The activation energy and sensitivity coefficient value of the samples is given in **Table 4**. With in-
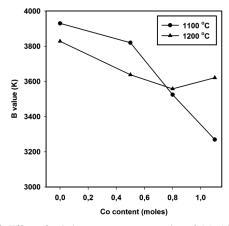

Figure 4: Effect of cobalt content on $B_{25/85}$ value of A1, A2, A6 and A10 samples sintered at 1100 and 1200 °C
Slika 4: Vpliv vsebnosti kobalta na vrednost $B_{25/85}$ vzorcev A1, A2, A6 in A10, sintranih na 1100 °C in na 1200 °C

creasing Co content, the $B_{25/85}$ constant and activation energy of the samples sintered at 1100 °C decreased from 3930 K to 3270 K and from 0.338 to 0.282 eV, respectively. A similar tendency was also seen in the A1, A2 and A6 samples sintered at 1200 °C. For the A10 sample, the $B_{25/85}$ constant and activation energy values were found to be 3620 K and 0.312 eV, respectively. The sensitivity coefficient value of all samples sintered at 1100 °C decreased from -4.426 to -3.683 %/K. When the sintering temperature increased to 1200 °C, the sensitivity coefficient value of all samples decreased from -4.311 to -4.078 %/K.

Table 4: The activation energy and sensitivity coefficient of A1, A2, A6 and A10 samples sintered at 1100 °C and 1200 °C for 5 h
Tabela 4: Aktivacijska energija in koeficient občutljivosti A1, A2, A6 in A10 vzorcev, sintranih 5 ur na 1100 °C in 1200 °C

Composition code	E_a (eV)		α_{25} (%/K)	
	1100 °C	1200 °C	1100 °C	1200 °C
A1	0.338	0.330	−4.426	−4.311
A2	0.329	0.313	−4.301	−4.097
A6	0.303	0.306	−3.970	−4.007
A10	0.282	0.312	−3.683	−4.078

4 DISCUSSION

The cubic spinel phase was found by XRD analysis in NiMn$_2$O$_4$ and Ni$_{0.5}$Co$_{0.8}$Mn$_{1.7}$O$_4$ samples sintered at 1100 °C for 5 h. No secondary phase was found in these samples. As it is well known from the binary phase diagram of Mn-Ni-O, the spinel phase can only form when the ratio of Ni/(Ni+Mn) is less than 0.35 at a calcination temperature of 900 °C.[11] The diffraction peaks of Ni$_{0.5}$Co$_{0.8}$Mn$_{1.7}$O$_4$ samples shift to the higher 2θ angles, indicating a decrease in the lattice parameter with the addition of Co$_3$O$_4$ due to the differences between the ionic radii of the Mn and Co ions. Wu et al.[12] reported that the peak shift toward higher 2θ angles with the increasing of Co content indicates lattice constriction when

Co substitutes Mn. It was also reported that the decrease in the lattice parameter with the addition of Co should be attributed to the fact that the ionic radius of Co^{2+} (0.072 nm) is smaller than that of Mn^{2+} (0.080 nm) for occupying the tetrahedral sites and/or Co^{3+} (0.068 nm) is smaller than Mn^{3+} (0.072 nm) for occupying the octahedral sites.[12,13] As can be seen in Figure 1, we observed a significant broadening and a decrease of the diffraction peak intensities in the XRD pattern of the $Ni_{0.5}Co_{0.8}Mn_{1.7}O_4$ sample. This could be attributed to a decrease in the average crystallite size as given in Table 2 due to the nano-size of the Co_3O_4 starting powder. Savic et al. reported that the increase in the diffraction peak width and the decrease in the peak intensities in the XRD patterns are associated with a decreasing of the crystallite size and an increasing of the strain.[14]

Since the desired NTC thermistor properties strongly depend on the densification and grain size, we also investigated the microstructure properties of these samples. The bulk density and grain size of the A1, A2, A6 and A10 samples sintered at 1100 °C were less than the samples sintered at 1200 °C. Smaller grains result in a large number of grain boundaries, which act as scattering centres for the flow of electrons and therefore higher electrical resistivity values were obtained when the samples were sintered at 1100 °C.[15] As expected, the increasing of the sintering temperature gave rise to an increase in the bulk density and the grain size of these samples, thus the room-temperature resistivity of the samples decreased. In addition, the cation distribution in the octahedral and tetrahedral sites changes with an increasing sintering temperature in the spinel ceramics. The ratio of Mn^{3+}/Mn^{4+} in the octahedral sites increases with the increasing sintering temperature and also results in a decrease in the resistivity.[16] The electrical resistivity of the samples decreased significantly with the increasing of the Co_3O_4 content. Muralidharan et al. observed that the resistivity and B-value decreased with the increasing Co content. Their observation is expected as the Co^{2+} and Co^{3+} ions can also occupy the octahedral sites and contribute to the electrical conductivity along with Mn^{3+}/Mn^{4+} ion pairs in the octahedral sites. This gives rise to a decrease of the resistivity, B-value and temperature coefficient of resistance.[2] This phenomenon is prominent for all samples sintered at 1100 °C, while the Co content was increasing in the samples. Similar trends were also observed for the A1, A2 and A6 compositions when the samples were sintered at 1200 °C. When the sintering temperature was increased from 1100 to 1200 °C for the A10 sample, similar resistivity values were found, but the B-values and activation energy of samples were nearly constant. Moreover, the lattice parameters were found to be 0.8365 nm and 0.8273 nm for the $NiMn_2O_4$ and $Ni_{0.5}Co_{0.8}Mn_{1.7}O_4$ samples, respectively. This may be due to the fact that the hopping distance of the charge carriers becomes easier with the decreasing lattice parameter, thus the resistivity value decreases.[17] The sensitivity coefficient and the activation-energy values of all the samples were found in the range –4.426 to –3.683 %/K and 0.282 eV to 0.338 eV, respectively. It is well known that the desired sensitivity coefficient, α_{25}, and the activation energy of the NTC thermistors are in the range –2.2 %/K to –5.5 %/K and 0.1–1.5 eV, respectively.[18,19]

5 CONCLUSION

The influence of nano-sized cobalt oxide additions on the structural and electrical properties of nickel-manganite-based NTC thermistors was investigated. Our results in this work indicate that a wide range of electrical properties of nickel-manganite-based NTC thermistors can be obtained by the addition of nano-sized cobalt oxide. The particularly interesting finding in this study demonstrated that the $Ni_{0.5}Co_{1.1}Mn_{1.4}O$ sample sintered at 1200 °C for 5 h has a low electrical resistivity and a high B-constant.

6 REFERENCES

[1] R. N. Jadhav, S. N. Mathad, V. Puri, Studies on the properties of $Ni_{0.6}Cu_{0.4}Mn_2O_4$ NTC ceramic due to Fe doping, Ceramics International, 38 (**2012**), 5181–5188, doi:10.1016/j.ceramint.2012. 03.024

[2] M. N. Muralidharan, P. R. Rohini, E. K. Sunny, K. R. Dayas, A. Seema, Effect of Cu and Fe addition on electrical properties of Ni–Mn–Co–O NTC thermistor compositions, Ceramics International, 38 (**2012**), 6481–6486, doi:10.1016/j.ceramint.2012. 05.025

[3] J. Fraden, Handbook of Modern Sensors Physics, Designs, and Applications, Springer Science+Business Media, New York 2010

[4] E. D. Macklen, Thermistors, Electrochemical Publications Limited, Scotland 1979

[5] K. Park, Fabrication and Electrical Properties of Mn-Ni-Co-Cu-Si Oxides Negative Temperature Coefficient Thermistors, Journal of the American Ceramic Society, 88 (**2005**), 862–866, doi:10.1111/ j.1551-2916.2005.00170.x

[6] J. Wang, J. Zhang, Effects of Mg substitution on microstructure and electrical properties of $NiMn_{2-x}Mg_xO_4$ NTC ceramics, Journal of Materials Research, 27 (**2012**), 928–931, doi:10.1557/jmr.2012.29

[7] K. Park, S. J. Kim, J. G. Kim, S. Nahm, Structural and electrical properties of MgO-doped $Mn_{1.4}Ni_{1.2}Co_{0.4-x}Mg_xO_4$ (0 = x = 0.25) NTC thermistors, Journal of the European Ceramic Society, 27 (**2007**), 2009–2016, doi:10.1016/j.jeurceramsoc.2006.07.002

[8] M. Hosseini, B. Yasaei, Effect of Grain Size and Microstructures on Resistivity of Mn-Co-Ni Thermistor, Ceramics International, 24 (**1998**), 543–545

[9] S. Talam, S. R. Karumuri, N. Gunnam, Synthesis, Characterization, and Spectroscopic Properties of ZnO Nanoparticles, ISRN Nanotechnology, 2012 (**2012**) 372505, 1–6, doi:10.5402/2012/372505

[10] A. Monshi, M. R. Foroughi., M. R. Monshi, Modified Scherrer Equation to Estimate More Accurately Nano-Crystallite Size Using XRD, World Journal of Nano Science and Engineering, 2 (**2012**), 154–160, doi:10.4236/wjnse.2012.23020

[11] M. N. Muralidharan, E. K. Sunny, K. R. Dayas, A. Seema, K. R. Resmi, Optimization of process parameters for the production of Ni–Mn–Co–Fe based NTC chip thermistors through tape casting route, Journal of Alloys and Compounds, 509 (**2011**), 9363–9371, doi:10.1016/j.jallcom.2011.07.037

[12] J. Wu, Z. Huang, Y. Hou, Y. Gao, J. Chu, Structural, electrical, and magnetic properties of $Mn_{2.52-x}Co_xNi_{0.48}O_4$ films, Journal of Applied Physics, 107 (**2010**) 053716, 1–6, doi:10.1063/1.3309780

[13] R. D. Shannon, Revised Effective Ionic Radii and Systematic Studies of Interatomic Distances in Halides and Chalcogenides, Acta Crystallography, A32 (**1976**), 751–767

[14] S. M. Savic, L. Mancic, K. Vojisavljevic, G. Stojanovic, Z. Brankovic, O. S. Aleksic, G. Brankovic, Microstructural and electrical changes in nickel manganite powder induced by mechanical activation, Materials Research Bulletin, 46 (**2011**), 1065–1071, doi:10.1016/j.materresbull.2011.03.008

[15] S. A. Kanade, V. Puri, Electrical properties of thick-film NTC thermistor composed of $Ni_{0.8}Co_{0.2}Mn_2O_4$ ceramic: Effect of inorganic oxide binder, Materials Research Bulletin, 43 (**2008**), 819–824, doi:10.1016/j.materresbull.2007.05.008

[16] W. Kong, L. Chen, B. Gao, B. Zhang, P. Zhao, G. Ji, A. Chang, C. Jiang, Fabrication and properties of $Mn_{1.56}Co_{0.96}Ni_{0.48}O_4$ free-standing ultrathin chips, Ceramics International, 40 (**2014**), 8405-8409, doi:10.1016/j.ceramint.2014.01.049

[17] C. Ma, Y. Liu, Y. Lu, H. Gao, H. Qian, J. Ding, Preparation and characterization of $Ni_{0.6}Mn_{2.4}O_4$ NTC ceramics by solid-state coordination reaction, Journal of Materials Science: Materials in Electronics, 24 (**2013**), 5183–5188, doi:10.1007/s10854-013-1542-2

[18] A. Feteira, Negative Temperature Coefficient Resistance (NTCR) Ceramic Thermistors: An Industrial Perspective, Journal of the American Ceramic Society, 92 (**2009**), 967–983, doi:10.1111/j.1551-2916.2009.02990.x

[19] K. Park, I. H. Han, Effect of Cr_2O_3 addition on the microstructure and electrical properties of Mn-Ni-Co oxides NTC thermistors, Journal of Electroceramics, 17 (**2006**), 1069–1073, doi:10.1007/s10832-006-8317-6